Estimating discharge from Landsat

Ryan M. Riggs (1), George H. Allen (1), Cédric H. David (2), Peirong Lin (3), Ming Pan (3), and Xiao Yang (4).

(1) Department of Geography, Texas A&M University, College Station, TX, USA, (2) Jet Propulsion Laboratory, California Institute of Technology, Pasadena, CA, USA, (3) Department of Civil & Environmental Engineering, Princeton University, Princeton, NJ, USA, (4) Department of Geological Sciences, University of North Carolina, Chapel Hill, NC, USA.

1. Key points

- Simple tool to produce estimates of Discharge
- Landsat widths can easily be extracted and converted into discharge estimates
- Characterization of discharge uncertainty allows for remote sensing measurements to be used for data assimilation

2. Why estimate discharge from Landsat?

Traditionally, river discharge has been measured using river gauges[1]. Due to the global decrease in publicly available gauge data over the last several decades, alternative approaches should be explored for monitoring river discharge[2]. Satellite remote sensing can help to fill this knowledge gap due to the temporally and spatially consistent sampling of rivers globally[3–5]. While there has been extensive development in this field over the last decade, most techniques are limited by spatial extent due to computational requirements[6–12] or by spatial resolution[13–15]. By leveraging the multidecadal archive of Landsat with global discharge estimates, we provide a Google Earth Engine (GEE) tool to make efficient and simple discharge estimates by anyone with access to GEE.

3. Data Products

We use Landsat 5, 7, and 8 imagery to calculate river widths and pair these widths with same-day discharge estimates from the Global Reach Level A-priori Discharge Estimates for SWOT (GRADES)[16]. GRADES is a global hydrologic dataset that contains daily discharge estimates at the reach scale from 1979-2014. By joining these two datasets, we create simple river width-discharge rating curves to efficiently estimate discharge across the Lower Mississippi Basin. This was selected for testing due to the large amount of validation data available.

4. Methods.

1. Acquire Landsat 5, 7, and 8 scenes for each river reach (Fig. 1a).
2. Apply the Dynamic Surface Water Extent (DSWE)[18] water classification algorithm to raw scenes (Fig. 1b).
3. Create a binary mask of river and non-river pixels using a cumulative cost function (Fig. 1c).
4. Intersect Global River Widths from Landsat (GRWL)[19] buffer with a 2 km buffer around point of interest (Fig. 1d).
5. Calculate the effective river width for each classified image.
6. Join same-day Landsat widths (1984-2013) and GRADES discharge estimates to produce a rating curve.
7. Use the rating curve to produce discharge estimates from 1984-2020 for each location.

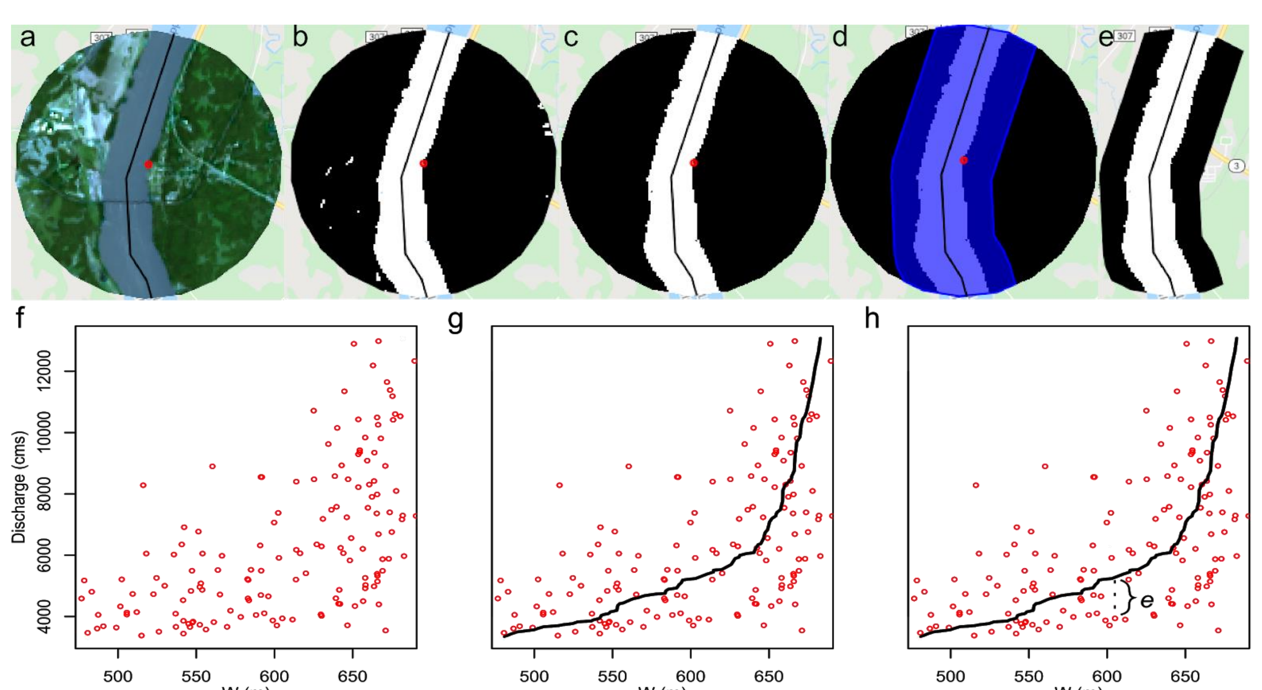

Figure 1. Steps followed to create a river mask for effective width measurement. The black centerline on all images in the GRWL dataset and the red point is the example discharge estimation location. **a**: Two-km buffer around the location of interest (red point). **b**: DSWE classified image. **c**: Remove non-river water pixels. **d**: Blue region is the intersecting geometry between the 2-km buffer and a buffer around the GRWL centerline. **e**: The region used to determine river width. **f**: Paired same-day RODEO widths and modelled discharge (red points). **g**: Rating curve (black line) developed from pairing quantile values of width and discharge. **h**: Estimated error is calculated as the difference from modelled discharge and RODEO discharge for each paired width (*e*).

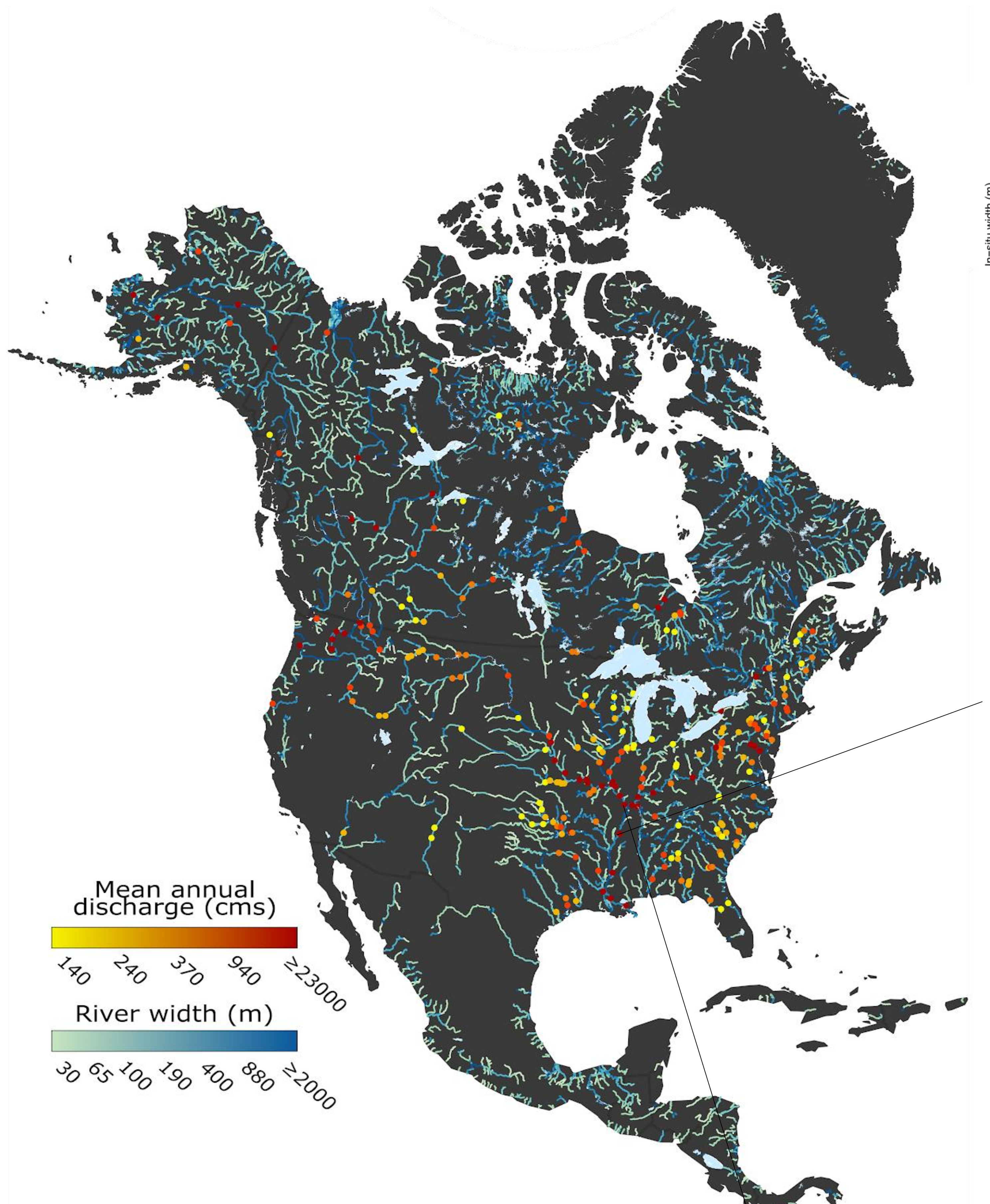

Figure 2. Mean annual discharge of the 242 USGS and GRDC gauges used in validation.

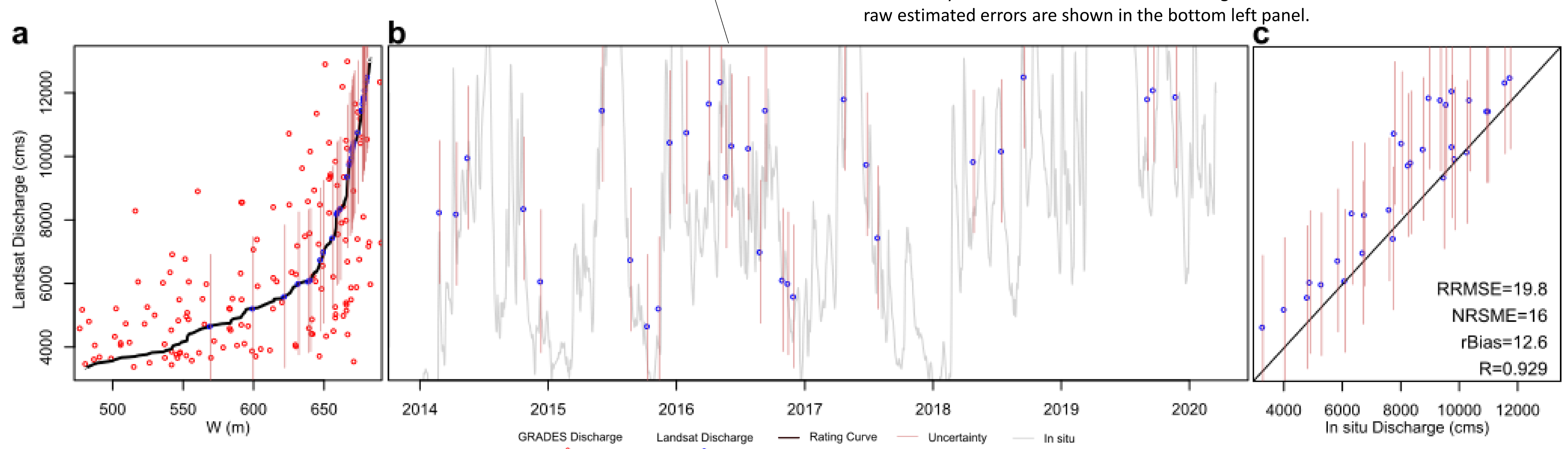

Figure 3. Sample USGS gauge location along the Mississippi River. Part A displays the paired GRADES-Landsat data used to create the rating curve along with Landsat discharge estimates from this rating curve. Part B displays a hydrograph of in situ data (gray) with the Landsat derived discharge estimates plotted in blue. Part C displays the comparison of same day in situ discharge measurements vs Landsat discharge estimates.

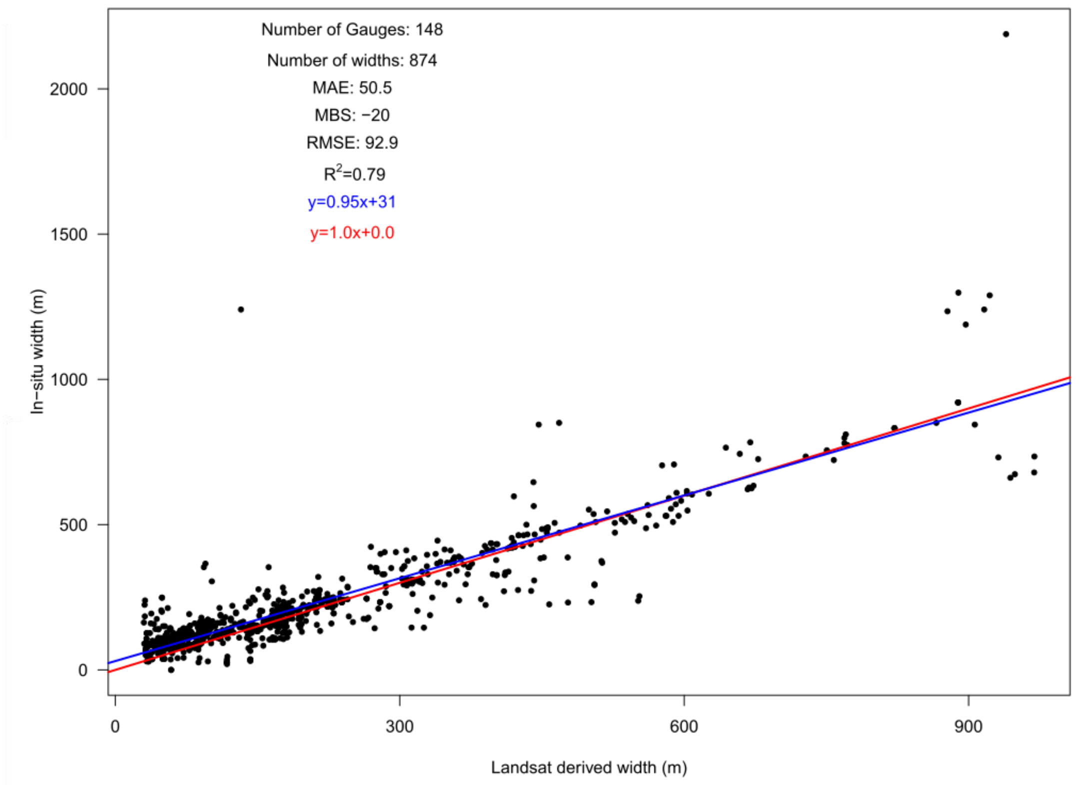

Figure 4. Width validation.

5. GEE Application

https://rriggs.users.earthengine.app/view/rodeo

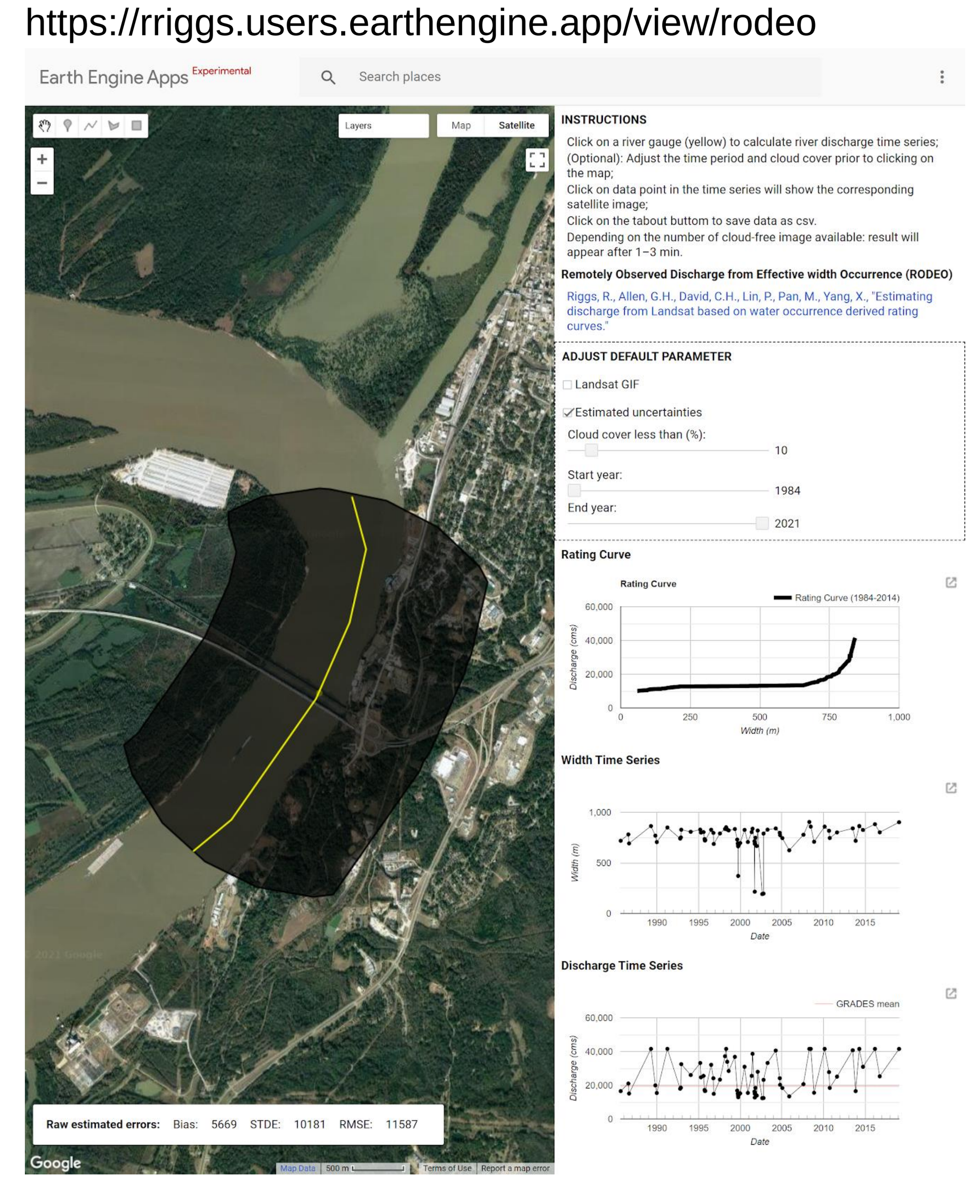

Figure 5. RODEO Google Earth Engine application running on the Mississippi River, Memphis, Tennessee. The GRWL centerline (yellow line) and buffer (dark gray polygon) are shown on the map. The parameters for the application are shown on the top right panel. The RODEO rating curve is shown on the next panel, followed by the width time series and discharge time series. The raw estimated errors are shown in the bottom left panel.

6. Discharge validation

Landsat derived discharges were validated using 242 USGS and GRDC gauges across North America. The validation period is from 2014-2020 due to all Landsat data from 1984-2013 being used to develop the rating curves.

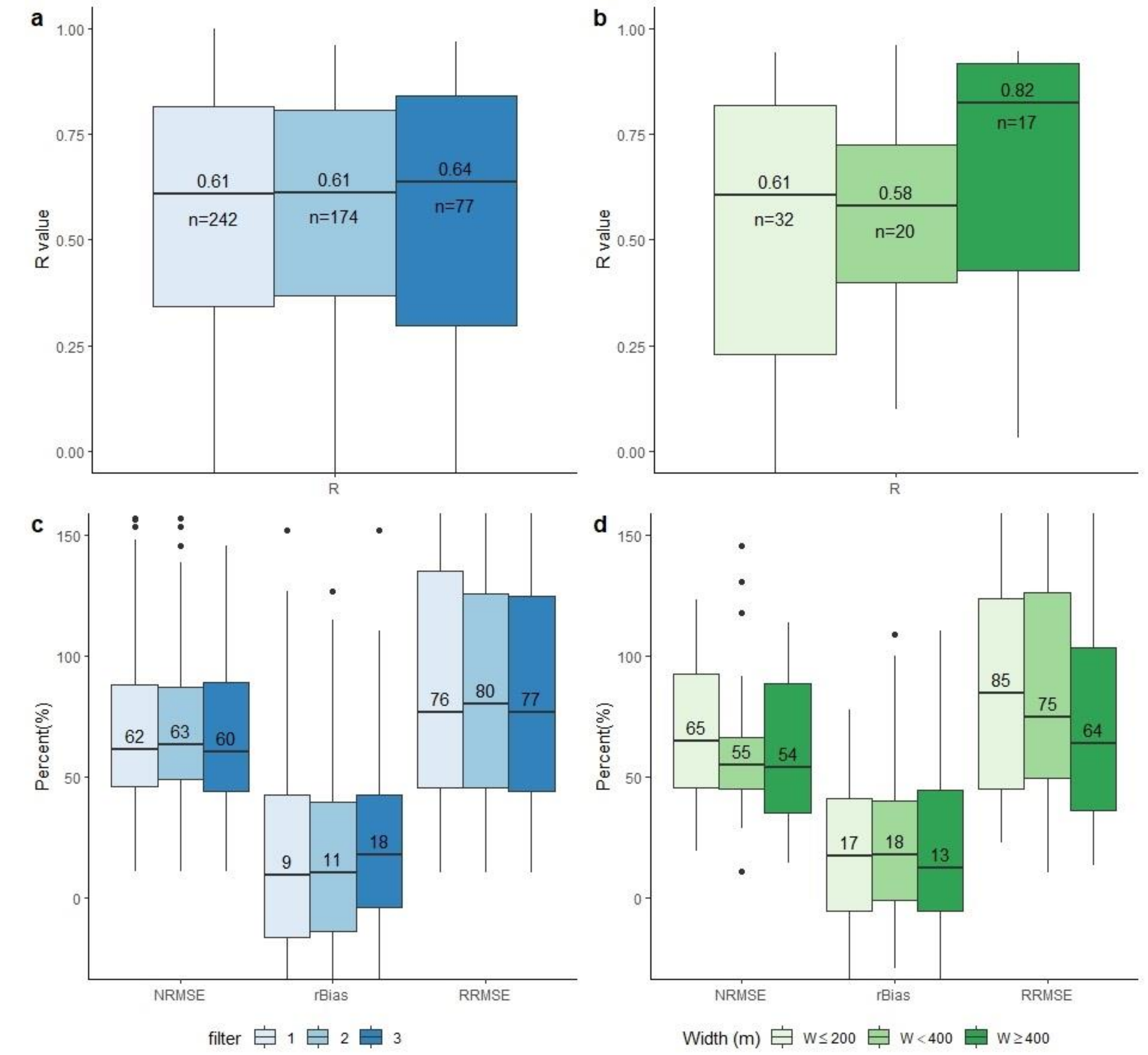

Figure 6. Boxplots displaying results for various gauge filters. The text above the black horizontal lines for each panel represents the median. **a:** R values for filters 1, 2, and 3, n is the number of gauges in each filter. **b:** R values for filter 3 gauges across various river width groupings, n is the number of gauges in each filter. **c:** The NRMSE, rBias, and RRMSE for gauge filters 1, 2, and 3. **d:** NRMSE, rBias, and RRMSE for various width groupings.

7. Acknowledgements

This study was funded by a NASA Terrestrial Hydrology Program Grant #NNH17ZDA001N-THP.

8. References

1. Dobriyal, P.; Badola, R.; Tuboi, C.; Hussain, S.A. A review of methods for monitoring streamflow for sustainable water resource management. Appl. Water Sci. 2017, 7, 2617–2628, doi:10.1007/s13201-016-0488-y.
2. Hannah, D.M.; Demuth, S.; Lanen, H.A.J. van; Looser, U.; Prudhomme, C.; Rees, G.; Stahl, K.; Tallaksen, L.M. Large-scale river flow archives: importance, current status and future needs. Hydrol. Process. 2011, 25, 1191–1200, doi:10.1002/hyp.7794.
3. Gleason, C.J.; Durand, M.T. Remote Sensing of River Discharge: A Review and a Framing for the Discipline. Remote Sens. 2020, 12, 1107, doi:10.3390/rs12071107.
4. Lettenmaier, D.P.; Alsdorf, D.; Dozier, J.; Huffman, G.J.; Pan, M.; Wood, E.F. Inroads of remote sensing into hydrologic science during the WRR era. Water Resour. Res. 2015, 51, 7309–7342, doi:10.1002/2015WR017616.
5. Smith, L.C. Satellite remote sensing of river inundation area, stage, and discharge: a review. Hydrol. Process. 1997, 11, 1427–1439, doi:10.1002/(SICI)1099-1085(199708)11:10<1427::AID-HYP473>3.0.CO;2-S.
6. Gleason, C.J.; Smith, L.C.; Lee, J. Retrieval of river discharge solely from satellite imagery and at-many-stations hydraulic geometry: Sensitivity to river form and optimization parameters. Water Resour. Res. 2014, 50, 9604–9619, doi:10.1002/2014WR016109.
7. Gleason, C.J.; Smith, L.C. Toward global mapping of river discharge using satellite images and at-many-stations hydraulic geometry. Proc. Natl. Acad. Sci. 2014, 111, 4788–4791, doi:10.1073/pnas.1317606111.
8. Garambois, P.-A.; Monnier, J. Inference of effective river properties from remotely sensed observations of water surface. Adv. Water Resour. 2015, 79, 103–120, doi:10.1016/j.advwatres.2015.02.007.
9. Durand, M.; Neal, J.; Rodríguez, E.; Andreadis, K.M.; Smith, L.C.; Yoon, Y. Estimating reach-averaged discharge for the River Severn from measurements of river water surface elevation and slope. J. Hydrol. 2014, 511, 92–104, doi:10.1016/j.jhydrol.2013.12.050.
10. Bonnema, M.G.; Sikder, S.; Hossain, F.; Durand, M.; Gleason, C.J.; Bjerklie, D.M. Benchmarking wide swath altimetry-based river discharge estimation algorithms for the Ganges river system. Water Resour. Res. 2016, 52, 2439–2461, doi:10.1002/2015WR017296.
11. Durand, M.; Gleason, C.J.; Garambois, P.A.; Bjerklie, D.; Smith, L.C.; Roux, H.; Rodriguez, E.; Bates, P.D.; Pavelsky, T.M.; Monnier, J.; et al. An intercomparison of remote sensing river discharge estimation algorithms from measurements of river height, width, and slope. Water Resour. Res. 2016, 52, 4527–4549, doi:10.1002/2015WR018434.
12. Hagemann, M.W.; Gleason, C.J.; Durand, M.T. BAM: Bayesian AMHG-Manning Inference of Discharge Using Remotely Sensed Stream Width, Slope, and Height. Water Resour. Res. 2017, 53, 9692–9707, doi:10.1002/2017WR021626.
13. Hou, J.; van Dijk, A.I.J.M.; Beck, H.E. Global satellite-based river gauging and the influence of river morphology on its application. Remote Sens. Environ. 2020, 239, 111629, doi:10.1016/j.rse.2019.111629.
14. Hou, J.; van Dijk, A.I.J.M.; Renzullo, L.J.; Vertessy, R.A. Using modelled discharge to develop satellite-based river gauging: a case study for the Amazon Basin. Hydrol. Earth Syst. Sci. 2018, 22, 6435–6448, doi:https://doi.org/10.5194/hess-22-6435-2018.
15. Tarpanelli, A.; Brocca, L.; Lacava, T.; Melone, F.; Moramarco, T.; Faruolo, M.; Pergola, N.; Tramutoli, V. Toward the estimation of river discharge variations using MODIS data in ungauged basins. Remote Sens. Environ. 2013, 136, 47–55, doi:10.1016/j.rse.2013.04.010.
16. Lin, P.; Pan, M.; Beck, H.E.; Yang, Y.; Yamazaki, D.; Frasson, R.; David, C.H.; Durand, M.; Pavelsky, T.M.; Allen, G.H.; et al. Global Reconstruction of Naturalized River Flows at 2.94 Million Reaches. Water Resour. Res. 2019, 55, 6499–6516, doi:10.1029/2019WR025287.
17. Reichle, R.H. Data assimilation methods in the Earth sciences. Adv. Water Resour. 2008, 31, 1411–1418, doi:10.1016/j.advwatres.2008.01.001.
18. Jones, J.W. Improved Automated Detection of Subpixel-Scale Inundation—Revised Dynamic Surface Water Extent (DSWE) Partial Surface Water Tests. Remote Sens. 2019, 11, 374, doi:10.3390/rs11040374.
19. Allen, G.H.; Pavelsky, T.M. Global extent of rivers and streams. Science 2018, 361, 585–588, doi:10.1126/science.aat0636.